



Research Article

Tropical cyclone intensity detection by geometric features of cyclone images and multilayer perceptron

Chinmoy Kar¹  · Ashirvad Kumar¹ · Sreeparna Banerjee²

© Springer Nature Switzerland AG 2019

Abstract

Tropical cyclone (TC) forecasting involves the prediction and intensity detection of a storm surge. TC intensity prediction and detection are important to minimize the loss of life and damage caused by TC. This paper proposes an image processing-based method to estimate the TC intensity from satellite images of tropical cyclones. The geometric features of TC images are used for the classification using the multilayer perceptron model. The proposed method classifies TC images over the Bay of Bengal and Arabian Sea with 84% accuracy.

Keywords Tropical cyclone · Cyclone eye · Prediction models · Multilayer perceptron

1 Introduction

A TC is said to be a high-speed rotating storm, characterized by a low-pressure centre with a closed low-level atmospheric movement of winds which produces heavy rain [1–4]. This may cause natural disaster, death and loss of property. A matured cyclone develops a centre called Eye associated with a ring of high intensity winds around it. According to researchers about 90% of the damage is due to flood by sea water formed by high intensity winds [3, 4].

TC's are observed from various observation centres worldwide [5]. Indian Meteorological Department (IMD) observes the tropical cyclones which are formed in the Arabian Sea (ARB) and Bay of Bengal (BoB) [5, 6]. The scale given in Table 1 [7] is used by IMD for cyclone classification.

The World Meteorological Organization Tropical Cyclone Programme is assigned to set up national and regionally coordinated systems to check that the damage or loss caused by TC [5]. Intensity of TCs is measured from these centres by a specific scale known as tropical cyclone intensity scale [8]. Various other techniques are

also established to predict the impact of a TC [9–16]. Dvorak technique [17] is a widely used method to detect cyclones using pattern recognition.

There are many techniques proposed by researchers towards intensity detection apart from Dvorak and modified Dvorak techniques [17–20]. Feature-based techniques [11, 12, 21, 22] are mostly focused on the geometric features of the TC images. Machine learning algorithms were introduced to solve many problems like image classification [12]. Earlier MLP algorithm used in order to predict the TC intensity [13, 14], but the approach proposed here depends on image based geometric features of TC. Intensity prediction using sea surface temperature is a popular method and many research works have been done in this area. A recent research attempt based on sea surface temperature is given in [23].

The TC eye detection is an important phase towards TC intensity detection [24]. TC eye is considered to be a unique area and is characterized by the cloud-free zone and is surrounded by thick cloud and weak wind [25]. Eye generally forms at the centre of Central Dense Overcast (CDO) region of storm and in most cases diameter

✉ Chinmoy Kar, chinmoy.k@smit.smu.edu.in; Ashirvad Kumar, ashirvadkumar8@gmail.com; Sreeparna Banerjee, sreeparnab@hotmail.com | ¹Department of Computer Science and Engineering, Sikkim Manipal Institute of Technology, Sikkim Manipal University, Gangtok, India. ²Department of Natural Science, Maulana Abul Kalam Azad University of Technology, Kolkata, India.



Table 1 Cyclone classification

S. no.	Name given due to intensity	Intensity
1	Depression	31–49 km/h (17–27 knots)
2	Deep depression	50–60 km/h (28–33 knots)
3	Cyclonic storm	62–87 km/h (34–47 knots)
4	Severe cyclonic storm	88–117 km/h (48–63 knots)
5	Very severe cyclonic storm	118–166 km/h (64–90 knots)
6	Extremely severe cyclonic storm	167–221 km/h (91–119 knots)

of the Eye of a storm is about 10–50 km. In the Dvorak technique [17], the presence of eye in satellite images are used for approximation of TC intensity.

The proposed model here is used to train and test the feature values of TC images through multilayer perceptron (MLP). MLP is considered to be a supervised learning technique [26]. MLP is a class of feed forward artificial neural network and it consists of input layer, output layer and at least one hidden layer. In MLP each node treated as a neuron which follows a non-linear activation function except for input nodes. It uses a supervised learning procedure called backpropagation algorithm and used for training and testing of the model [22].

In this paper Sect. 2 describes the dataset. Section 3 describes the methods and implementation details of the proposed algorithm. Section 4 is devoted to results and discussion and Sect. 5 concludes the proposed work.

2 Datasets

TC images are collected from Institute of Meteorological Satellite Studies [27] and IMD [28]. The images were taken from satellite known as INSAT 3D, Kalpana1 and Meteosat-7 (Fig. 1). The complete dataset is divided into the three categories based on the intensity (Table 1).

3 Methodology and implementation

There following steps are taken for model formulation and implementation:

- (a) Image recognition process
- (b) Pre-processing of TC images
- (c) Feature extraction from TC images
- (d) Training and testing through MLP

Block diagram of the proposed system is given Fig. 2.

- (a) Collection of TC images

TC images are collected from the dataset mentioned in Sect. 2. Further, images are categorized based on various classes referred in Table 1.

- (b) Pre-processing of TC images

In the pre-processing step, images are cropped based on ROI. Here images of D, CS and ESCS are passes through

Fig. 1 TC image of ESCS and CS [27]

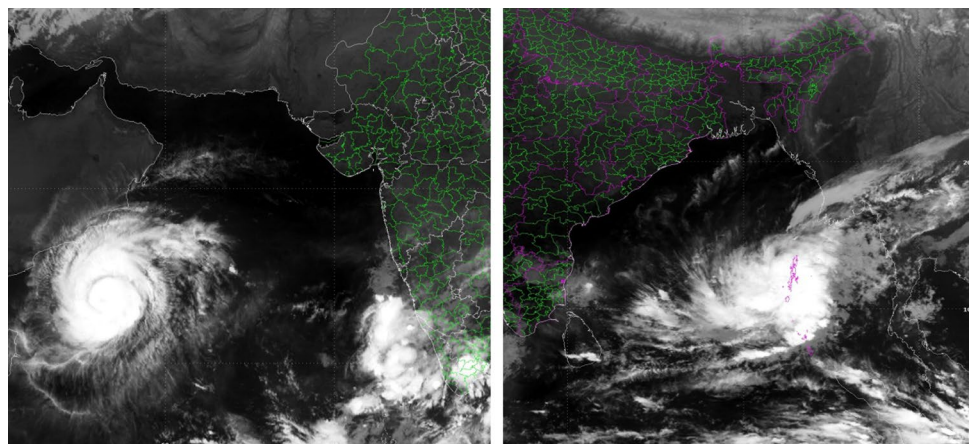


Fig. 2 Block diagram of proposed methodology



Gaussian blur or Gaussian smoothing to remove the noise (Fig. 3).

(c) Features extraction from TC images

Mean (M), variance (V), density (D), decentricity (DC), area of cyclone (AC) and area of eye (AE) are extracted from a TC image. First, Centre of Gravity (CoG) needs to be calculated based on work done by Onodera [29] for finding the features such as mean, variance (V), density (D), decentricity (DC) [10, 11, 29, 30]. The following formulas are used on image I of size $m \times n$ to calculate the CoG:

$$i_{cog} = \left(\sum_{i=1}^m \sum_{j=1}^n i * I_{ij} \right) / \left(\sum_{i=1}^m \sum_{j=1}^n I_{ij} \right) \tag{1}$$

$$j_{cog} = \left(\sum_{i=1}^m \sum_{j=1}^n j * I_{ij} \right) / \left(\sum_{i=1}^m \sum_{j=1}^n I_{ij} \right) \tag{2}$$

The parameters stated above are used further to find area of cyclone over original image (AC) and area of eye (AE) which are formulated exclusively for this work.

$$AC = \pi \times (ed_{max})^2 \tag{3}$$

$$AE = \pi \times (ed_k)^2 \tag{4}$$

$$ed_{ij} = \sqrt{(i - i_{cog})^2 + (j - j_{cog})^2} \tag{5}$$

$$M = \frac{1}{n} \sum_{k=1}^n \frac{ed_k}{ed_{max}} \tag{6}$$

$$V = \frac{1}{n - 1} \sum_{k=1}^n \left(\frac{ed_k}{ed_{max}} - M \right)^2 \tag{7}$$

$$D = \frac{1}{(\pi * ed_{max})^2} \times \left(\sum_{i=1}^m \sum_{j=1}^n I_{ij} \right) \tag{8}$$

$$DC = \frac{ed_{min}}{ed_{max}} \tag{9}$$

The Table 2 stated below summarises the features used for proposed work.

(d) Multilayer perceptron for training and testing:

MLP is an artificial neural network which is used to train and test the proposed model. MLP is a feedforward network with one or more hidden layers [31]. It uses backpropagation algorithm for finding the gradient (Fig. 4).

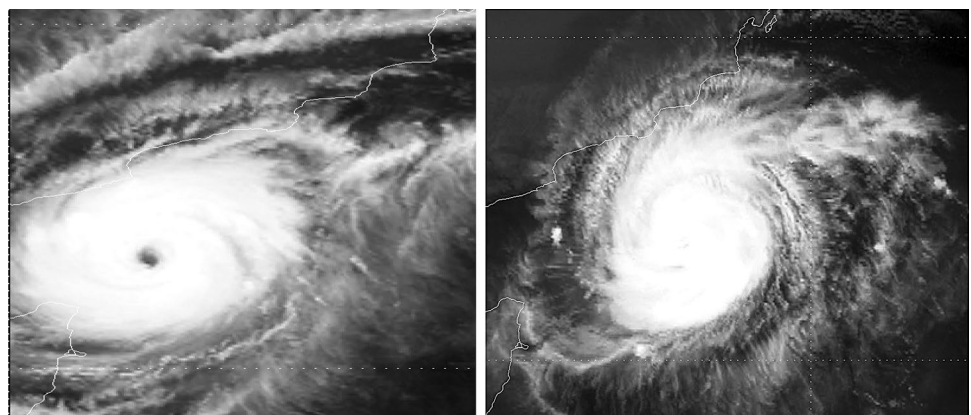
In MLP the gradient is determined by the backpropagation algorithm. The change in weight is calculated by multiplying the gradient with the learning rate and added to the previous change in the weight multiplied by momentum. The standard formula for perceptron learning is given below:

$$v(x) = \frac{1}{1 + e^{-ax}} \tag{10}$$

Table 2 Features of the TC image

S. no.	Feature name	Expression
1	Mean (M)	$M = \frac{1}{n} \sum_{k=1}^n \frac{ed_k}{ed_{max}}$
2	Variance (V)	$V = \frac{1}{n - 1} \sum_{k=1}^n \left(\frac{ed_k}{ed_{max}} - M \right)^2$
3	Density (D)	$D = \frac{1}{(\pi * ed_{max})^2} \times \left(\sum_{i=1}^m \sum_{j=1}^n I_{ij} \right)$
4	Decentricity (DC)	$DC = \frac{ed_{min}}{ed_{max}}$
5	Area of cyclone over original image (AC)	$AC = \pi \times (ed_{max})^2$
6	Area of eye (AE)	$AE = \pi \times (ed_k)^2$

Fig. 3 Figure after the ROI detection



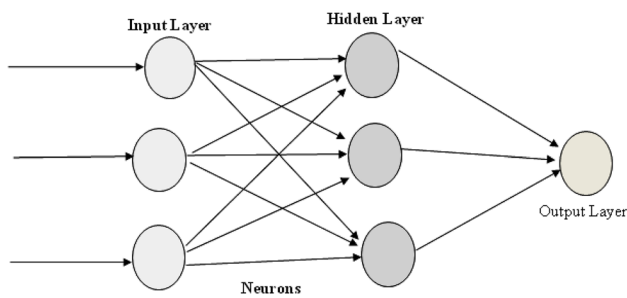


Fig. 4 Architecture of multilayer perceptron [31]

The above-mentioned sigmoid function is used as an activation function where $0 < u(x) < 1$, a is a constant to control the activation function.

The error function for each unknown training pattern p is calculated based on following formula:

$$r_p = \sum_{i=1}^n (o_{ip} - t_{ip})^2 \tag{11}$$

where r_p is the error calculated based on output o_{ip} and target t_{ip} .

The purpose of backpropagation algorithm is to minimize the error gradually by adjusting the weight values.

$$w_{(next)} = w + \Delta w \tag{12}$$

$$\Delta w = \eta \times G + \alpha \times \Delta w_{(previous)} \tag{13}$$

Here, η is learning rate $0 < \eta < 1$, G is gradient and α stands for momentum factor $0 < \alpha < 1$.

4 Testing and result analysis

In this project we have used Octave GNU version 4.2.0 for the feature extraction whereas we have used Weka for the training and testing purposes and the version of Weka is 3.8.

(a) Octave GNU

Octave GNU version 4.2.0 is open source software [32] used for feature extraction using image processing techniques.

(b) Weka

Weka version 3.8 [33] is a collection of machine learning techniques for data mining and other activities. The feature values are used in Weka to train and test the model through MLP.

(c) Discussion on results of MLP

The result of Multilayer layer perceptron (MLP) is comparable with other feature-based methods. Accuracy of MLP is approximately 84% in tenfold cross validation test. The test results in a 66% split in MLP is 83%, which is given in the Table 3.

Receiver operating characteristic curve (ROC) is a graphical representation of true positive rate (TPR) against the false positive rate (FPR). ROC curve is used to illustrate the diagnostic capability of a classifier. The following formulas are associated with ROC curve.

$$TPR = \frac{TP}{TP + FN} \tag{14}$$

Table 3 Summary of test results

Attributes	Test mode	Values MLP	
Correctly classified instances	Tenfold cross-validation	83.6412%	
Incorrectly classified instances		16.3588%	
Kappa statistic		0.734	
Mean absolute error		0.1392	
Root mean squared error		0.2895	
Relative absolute error		33.997%	
Root relative squared error		64.0036%	
Correctly classified instances		Split 66.0% train, remainder test	82.9457%
Incorrectly classified instances			17.0543%
Kappa statistic			0.7255
Mean absolute error	0.142		
Root mean squared error	0.3034		
Relative absolute error	34.5189%		
Root relative squared error	66.518%		

$$TPR = \frac{FP}{FP + TN} \tag{15}$$

where true positive (TP), true negative (TN), false positive (FP), false negative (FN) (Table 4).

Table 4 (a) Summary of test results confusion matrix for test mode: tenfold cross-validation, (b) confusion matrix for test mode: 66% split

Name of the classifier	Classified as			Classes
	ESCS	CS	D	
(a) MLP	64	9	0	ESCS
	19	167	8	CS
	4	22	86	D
(b) MLP	24	3	0	ESCS
	6	55	3	CS
	1	9	28	D

The ROC curves shown in Figs. 5 and 6 represent the performance of MLP in tenfold cross validation and 66% split. The performance of MLP in 66% split is better than tenfold cross validation.

5 Conclusion

The MLP technique with geometric features turned out to be useful for the detection of cyclone intensity. In comparison with the conventional method like Dvorak Technique and other standard methods, this method works fine on ESCS, CS and D cyclones. The proposed method is completely based on images and its geometric property with accuracy around 84%. This proposed method is highly inspired by the work done on feature vectors of [10, 11]. The detection method is solely based on the images such as ESCS, CS and D which have been analysed in the results section. Below is a comparison made between other feature-based TC intensity detection techniques with our proposed method.

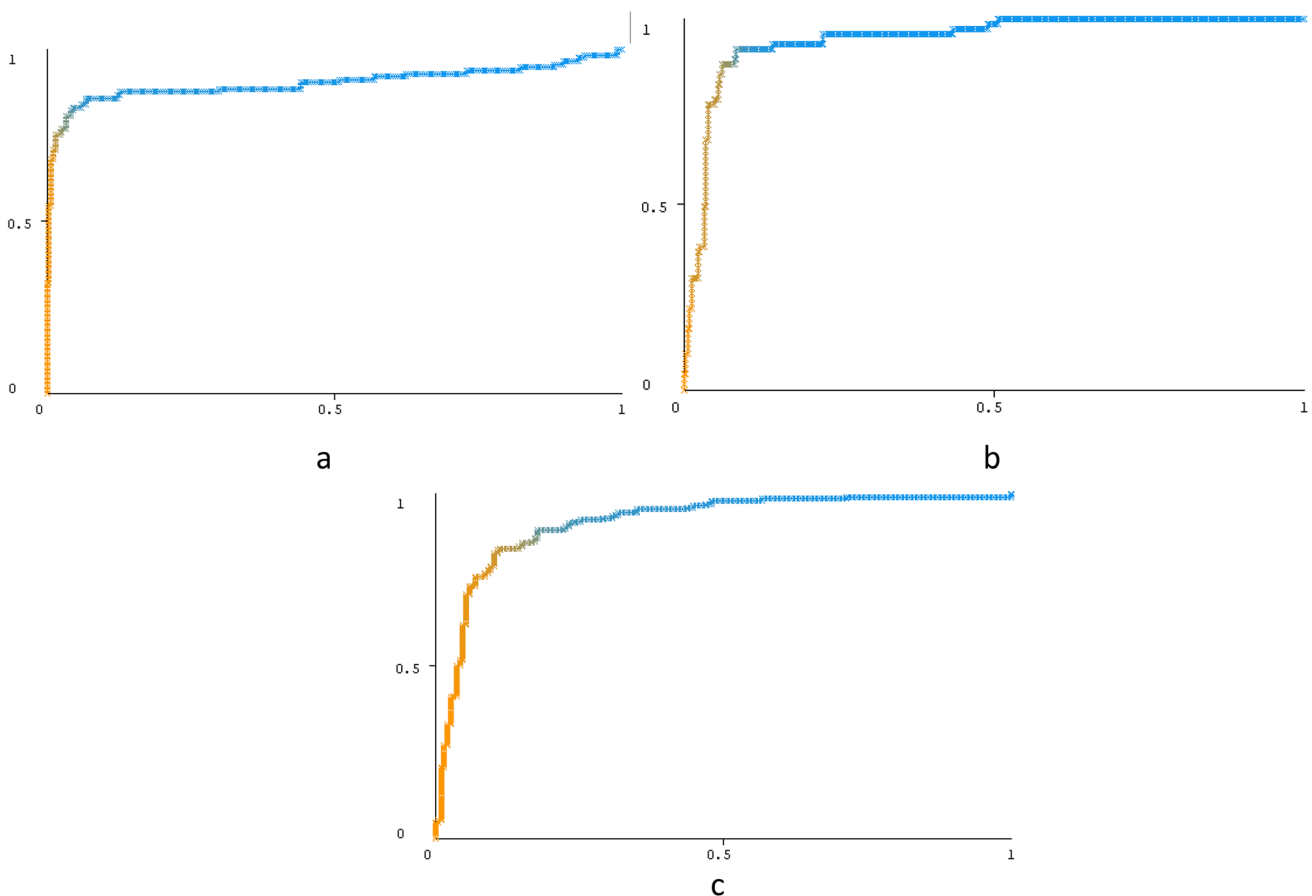


Fig. 5 ROC curves tenfold cross-validation (X axis FPR, Y axis TPR). **a** Class value: D area under ROC=0.9005, **b** class value: ESCS area under ROC=0.9446, **c** class value: CS area under ROC=0.9136

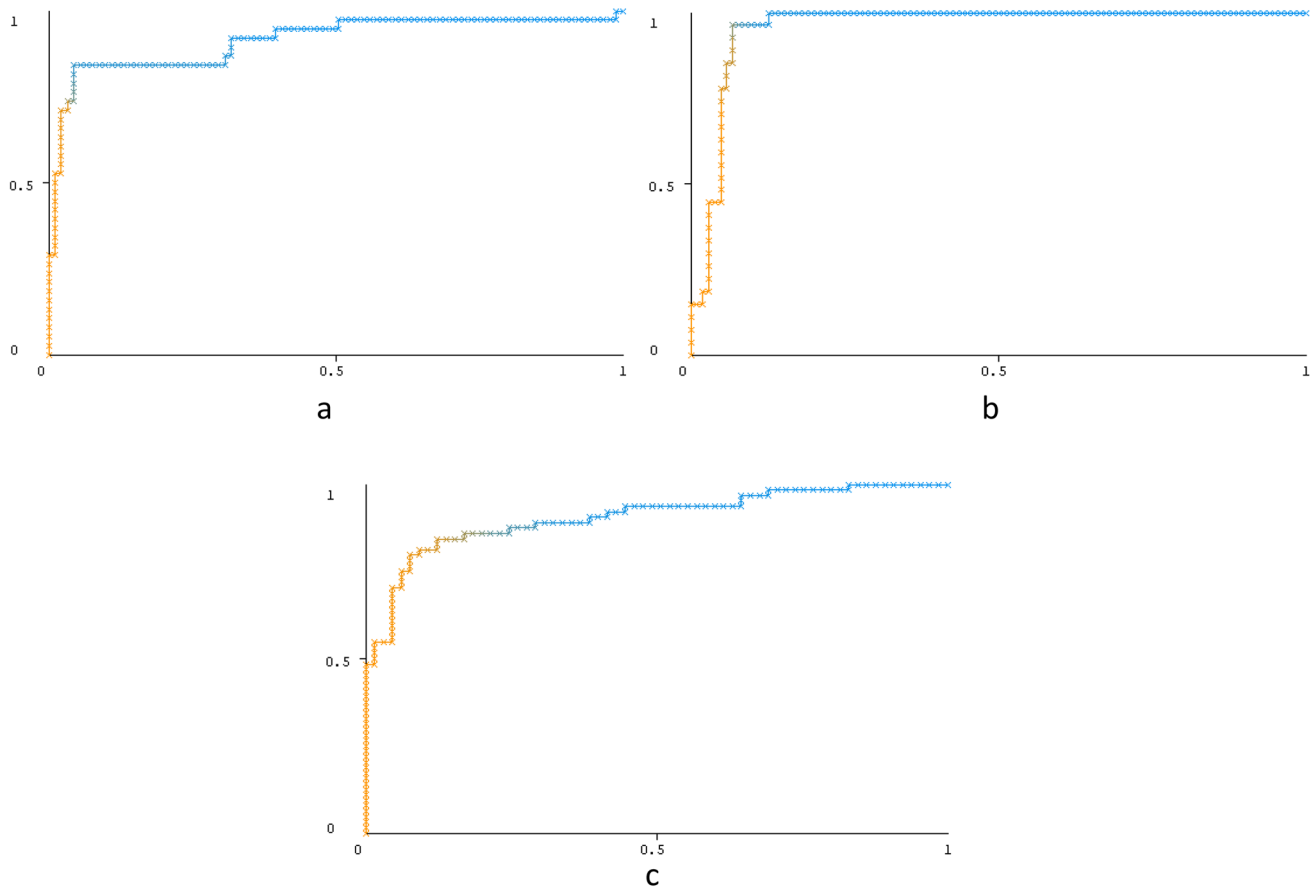


Fig. 6 ROC curves 66% split (X axis FPR, Y axis TPR). **a** Class value: D area under ROC=0.9005, **b** class value: ESCS area under ROC=0.9586, **c** class value: CS area under ROC =0.9055

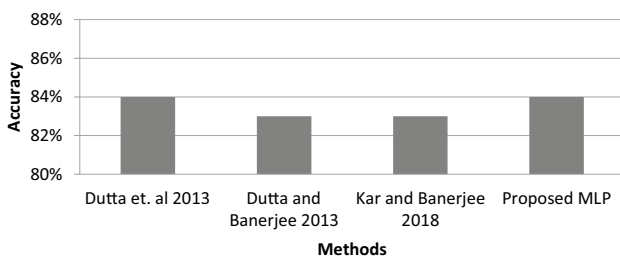


Fig. 7 Comparison between various methods

The other methods compared here (Fig. 7) are also tested on similar type of images and environment. Moreover, the number of images used here is greater than the work done in [10, 11]. The proposed method also compared with the work done by Pradhan et al. [12], where the performance of deep convolution network is varying from 80.66 to 95.47% and 76.91 to 92.55% depending upon datasets. The number of cyclone images of ESCS, CS and D classes is 379. The proposed work is restricted

on ESCS, CS, and D type of images and to be extended further with other classes such as DD, ECS, and VSCS.

Acknowledgements Institute of Meteorological Satellite Studies, Space Science and Engineering Centre, University of Wisconsin-Madison (<http://tropic.ssec.wisc.edu>) and Meteorological Center, Indian Meteorological Department (<http://satellite.imd.gov.in/insat.htm>).

Compliance with ethical standards

Conflict of interest The authors declare that they have no conflict of interest.

References

1. Regional Specialized Meteorological Centre for Tropical Cyclones over North Indian Ocean, IMD Frequently asked Question. <http://www.rsmcnewdelhi.imd.gov.in/images/-pdf/cyclone-awareness/terminology/faq.pdf>. Accessed 1 Aug 2019
2. Hurricane Research Division, NOAA. <https://www.aoml.noaa.gov/hrd/tcfaq/A1.html>. Accessed 25 July 2019
3. Dube SK, Rao AD, Sinha PC, Murty TS, Bahulayan N (1997) Storm surge in the Bay of Bengal and Arabian Sea: the problem and its prediction. *Mausam* 48:283–304

4. Dube SK, Jain I, Rao A, Murty T (2009) Storm surge modelling for the Bay of Bengal and Arabian Sea. *Nat Hazards* 51:3–27. <https://doi.org/10.1007/s11069-009-9397-9>
5. Worldwide Tropical Cyclone Centers. <https://www.nhc.noaa.gov/abouttrsmc.shtml>. Accessed 1 Aug 2019
6. <http://www.rsmcnewdelhi.imd.gov.in/index.php?lang=en>. Accessed 1 Aug 2019
7. WMO/ESCAP Panel on Tropical Cyclones (2015) Tropical cyclone operational plan for the Bay of Bengal and the Arabian Sea 2015 (report no. TCP-21). World Meteorological Organization, March 2015, pp 11–12
8. https://en.wikipedia.org/wiki/Tropical_cyclone_scales. Accessed 1 Aug 2019
9. Dube SK, Chittibabu P, Sinha PC et al (2004) Numerical modelling of storm surge in the head Bay of Bengal using location specific model. *Nat Hazards* 31:437. <https://doi.org/10.1023/B:NHAZ.0000023361.94609.4a>
10. Kar C, Banerjee S (2018) An image processing approach for intensity detection of tropical cyclone using feature vector analysis. *Int J Image Data Fusion* 9(4):338–348. <https://doi.org/10.1080/19479832.2018.1491896>
11. Kar C, Banerjee S (2016) An approach towards automatic intensity detection of tropical cyclone by weight based unique feature vector. In: IEEE international conference on computational intelligence and computing research (ICIC), Chennai, 2016, pp 1–4
12. Pradhan R, Aygun R, Maskey S et al (2018) Tropical cyclone intensity estimation using a deep convolutional neural network. *IEEE Trans Image Process* 27(2):692–702. <https://doi.org/10.1109/TIP.2017.2766358>
13. Chaudhuri S, Dutta D, Goswami S, Middey A (2012) Intensity forecast of tropical cyclones over North Indian Ocean using multilayer perceptron model: skill and performance verification. *Nat Hazards*. <https://doi.org/10.1007/s11069-012-0346-7>
14. Chaudhuri S, Goswami S, Middey A (2014) Medium range forecast of cyclogenesis over North Indian Ocean with multi-layer perceptron model using satellite data. *Nat Hazards* 70:173–193. <https://doi.org/10.1007/s11069-013-0805-9>
15. Dutta I, Banerjee S, De M (2013) An algorithm for pre-processing of satellite images of cyclone clouds. *Int J Comput Appl* 78:13–17. <https://doi.org/10.5120/13598-1317>
16. Dutta I, Banerjee S (2013) Elliptic Fourier descriptors in the study of cyclone cloud intensity patterns. *Int J Image Process* 7(4):402–417
17. Dvorak VF (1975) Tropical cyclone intensity analysis and forecasting from satellite imagery. *Mon Weather Rev* 103:420–430
18. Knaff JA, Brown DP, Courtney J, Gallina GM, Bevan JL II (2010) An evaluation of Dvorak technique-based tropical cyclone intensity estimates. *Weather Forecast* 25:1362–1379. <https://doi.org/10.1175/2010WAF222375.1>
19. Manion A, Evans C, Olander TL et al (2015) An evaluation of advanced Dvorak technique-derived tropical cyclone intensity estimates during extratropical transition using synthetic satellite imagery. *Weather Forecast* 30:984–1009. <https://doi.org/10.1175/WAF-D-15-0019.1>
20. Dvorak VF (1984) Tropical cyclone intensity analysis using satellite data. NOAA Tech. Rep. NESDIS 11. http://severe.worldweath.er.wmo.int/TCFW/RAI_Training/Dvorak_1984.pdf. Accessed 1 Aug 2019
21. Karimi V, Tashk A (2012) Age and gender estimation by using hybrid facial features. In: 20th telecommunications forum (TELFOR), Belgrade, 2012, pp 1725–1728. <https://doi.org/10.1109/TELFOR.2012.6419560>
22. Hoang ND, Nguyen QL, Tran XL (2019) Automatic detection of concrete spalling using piecewise linear stochastic gradient descent logistic regression and image texture analysis. *Complexity*. <https://doi.org/10.1155/2019/5910625>
23. Sharma AK, Prasad V, Kumar R, Sharma A (2018) Analysis on the occurrence of tropical cyclone in the South Pacific region using recurrent neural network with LSTM. In: Neural information processing. ICONIP 2018. Lecture notes in computer science, vol 11301
24. Knaff JA, Demaria RT (2017) Forecasting tropical cyclone eye formation and dissipation in infrared imagery. *Weather Forecast* 32:2103–2116. <https://doi.org/10.1175/WAF-D-17-0037.1>
25. http://www.imd.gov.in/pages/services_cyclone.php. Accessed 2 Apr 2019
26. Popescu MC, Valentina E, Balas M, Popescu L, Mastorakis N (2009) Multilayer perceptron and neural networks. *WSEAS Trans Circuits Syst* 8(7):579–588
27. Institute of Meteorological Satellite Studies, Space Science and Engineering Center, University of Wisconsin-Madison. <http://tropic.ssec.wisc.edu/>
28. National Satellite Meteorological Center, Archived Images, Indian Meteorological Department. <http://satellite.imd.gov.in/insat.htm>. Accessed 22 Jan 2019
29. Onodera Y, Watanabe H, Taguchi A et al (2002) Translation and rotation-invariant pattern recognition method using neural network with back-propagation. In: Communications on the move Singapore 'ICCS/ISITA'92, 16–20 November 1992. IEEE, Singapore, pp 548–552. <https://doi.org/10.1109/ICCS.1992.254891>
30. Barnes D, Manic M (2010). STRICR-FB, a novel size–translation–rotation-invariant character recognition method. In: 3rd international conference on human system interaction. IEEE, Poland, pp 163–168
31. Wilson E, Tufts DW (1994) Multilayer perceptron design algorithm. In: IEEE workshop on neural networks for signal processing, Ermioni, Greece, pp 61–68. <https://doi.org/10.1109/nnspp.1994.366063>
32. Eaton JW, Bateman D, Hauberg S, Wehbring R (2016) GNU Octave version 4.2.0 manual: a high-level interactive language for numerical computations. <http://www.gnu.org/software/octave/doc/interpreter/>. Accessed 1 Aug 2019
33. Frank E, Hall MA, Witten IH (2016) The WEKA workbench. Online appendix for data mining: practical machine learning tools and techniques, 4th edn. Morgan Kaufmann, Burlington

Publisher's Note Springer Nature remains neutral with regard to jurisdictional claims in published maps and institutional affiliations.